Up states are rare in awake auditory cortex

Tomás Hromádka, Anthony M. Zador and Michael R. DeWeese

J Neurophysiol 109:1989-1995, 2013. First published 23 January 2013;
doi: 10.1152/jn.00600.2012

Journal of Neurophysiology publishes original articles on the function of the nervous system. It is published 24 times a year (twice monthly) by the American Physiological Society, 9650 Rockville Pike, Bethesda MD 20814-3991. ESSN: 1522-1598. Visit our website at http://www.the-aps.org/.

J Neurophysiol 109: 1989–1995, 2013.
First published January 23, 2013; doi:10.1152/jn.00600.2012.

Up states are rare in awake auditory cortex

Tomáš Hromádka,[1] Anthony M. Zador,[1] and Michael R. DeWeese[1,2]

[1]*Cold Spring Harbor Laboratory, Cold Spring Harbor, New York; and* [2]*Department of Physics, Helen Wills Neuroscience Institute, and the Redwood Center for Theoretical Neuroscience, University of California, Berkeley, California*

Submitted 20 July 2012; accepted in final form 22 January 2013

Hromádka T, Zador AM, DeWeese MR. Up states are rare in awake auditory cortex. *J Neurophysiol* 109: 1989–1995, 2013. First published January 23, 2013; doi:10.1152/jn.00600.2012.—The dynamics of subthreshold membrane potential provide insight into the organization of activity in neural circuits. In many brain areas, membrane potential is bistable, transiting between a relatively hyperpolarized down state and a depolarized up state. These up and down states, which have been proposed to play a number of computational roles, have mainly been studied in anesthetized and in vitro preparations. Here, we have used intracellular recordings to characterize the dynamics of membrane potential in the auditory cortex of awake rats. We find that long up states are rare in the awake auditory cortex, with only 0.4% of up states >500 ms. Most neurons displayed only brief up states (bumps) and spent on average ~1% of recording time in up states >500 ms. We suggest that the near absence of long up states in awake auditory cortex may reflect an adaptation to the rapid processing of auditory stimuli.

awake auditory cortex; electrophysiology; membrane potential

FLUCTUATIONS IN MEMBRANE POTENTIAL of single neurons provide a window into the dynamics of neuronal networks. Up and down states, the bistability of the neuronal membrane potential, were first described in unanesthetized striatum (Wilson and Groves 1981) and attracted considerable attention as they have been suggested to underlie persistent activity in cortical networks (McCormick et al. 2003; Wang 2001). Since then, however, up and down states have been studied and described mostly in anesthetized preparations (or in vitro) in various cortical areas (Carandini and Ferster 1997; Lampl et al. 1999; Margrie and Schaefer 2003; Metherate and Ashe 1993; Sanchez-Vives and McCormick 2000; Steriade et al. 1993a; Stern et al. 1997). Despite being studied in many cortical areas, up and down states have not always been observed (Anderson et al. 2000; Bruno and Sakmann 2006; DeWeese and Zador 2006; Wilent and Contreras 2005). The few studies describing up and down states in unanesthetized preparations revealed a dependence on behavioral state (Crochet and Petersen 2006; Gentet et al. 2010; Okun et al. 2010; Steriade et al. 2001; Timofeev et al. 2001).

Lack of universally agreed-on definition of what constitutes an up or down state hinders comparison of membrane potential dynamics across brain regions. Although up states were originally defined on the basis of intracellular activity (Wilson and Groves 1981), their presence is now commonly inferred using extracellular population spiking activity (Luczak et al. 2007) or local field potentials (LFPs; Haslinger et al. 2006) as a proxy, often in the anesthetized animal. Thus the prevalence of up and down states in the awake cortex remains controversial for most brain areas, including the auditory cortex.

We have previously reported that prolonged up and down states are not observed in the auditory cortex of anesthetized rats (DeWeese and Zador 2006). Here, we extend those observations to the auditory cortex of awake animals. We find that long up states are rare in awake auditory cortex with only 0.4% of up states >500 ms. Most neurons underwent only transient depolarizations, which would not be well-characterized as up states, and spent most of the time near the resting potential, spending ~1% of recording time on average in up states >500 ms. As a control, we present traces from neurons recorded in another brain region [posterior parietal cortex (PPC)] of anesthetized rats using the same recording methods, demonstrating that our recording techniques and analyses do detect long up states during two-state behavior when and if it is present.

MATERIALS AND METHODS

Surgery. Sprague-Dawley rats (13 animals, 24–30 days old) underwent surgery in strict accordance with the National Institutes of Health guidelines, as approved by the Cold Spring Harbor Laboratory Animal Care and Use Committee. A small craniotomy and durotomy were performed over the left auditory cortex, protected by a plastic recording well with removable cap. The position of the craniotomy was determined by its distance from bregma (4.5 mm posterior and 4 mm lateral). LFPs and single-unit spiking responses were recorded during the same recording sessions as some of our whole cell recordings. For these cases, and for all of our whole cell recordings in auditory cortex, when clear auditory responses were observed, they exhibited short latencies consistent with recordings from primary auditory cortex (A1). Based on these anatomic landmarks and physiological observations, we expect that the majority of recordings were performed in A1 (Doron et al. 2002; see also Hromádka et al. 2008), although some may have been from the anterior auditory field. An aluminum headpost was attached to the skull with RelyX Luting Cement (3M ESPE, St. Paul, MN). A silver chloride ground wire was implanted subcutaneously on the back of the animal. Between recording sessions, the brain surface was covered with Kwik-Cast (World Precision Instruments, Sarasota, FL). During recording sessions, the plastic cap and Kwik-Cast layer were removed, and the cortex was covered with physiological buffer (in mM: 127 NaCl, 25 Na_2CO_3, 1.25 NaH_2PO_4, 2.5 KCl, 1 $MgCl_2$, and 25 glucose) mixed with 1.5% agar.

Two recordings were obtained from PPC of rats (Nakamura 1999) anesthetized with ketamine (60 mg/kg) and medetomidine (0.5 mg/kg).

Electrophysiology. Recordings were obtained using standard blind whole cell recording technique (DeWeese et al. 2003; Machens et al. 2004; Wehr and Zador 2003). Electrodes were pulled from filamented, thin-walled, borosilicate glass (outer diameter, 1.5 mm; inner diameter, 1.17 mm; World Precision Instruments) on a vertical two-stage puller (Narishige, East Meadow, NY). For recording, electrodes were filled with internal solution containing (in mM): 10 KCl, 140 K-

Address for reprint requests and other correspondence: M. R. DeWeese, Dept. of Physics and Helen Wills Neuroscience Institute, Univ. of California, Berkeley, CA 94720-3190 (e-mail: deweese@berkeley.edu).

gluconate, 10 HEPES, 2 $MgCl_2$, 0.05 $CaCl_2$, 4 MgATP, 0.4 Na_2GTP, 10 Na_2-phosphocreatine, 10 BAPTA, and 1% biocytin, pH 7.25, diluted to 290 mOsm. Resistance to bath was 3.5–5.0 MΩ before seal formation. Recordings were obtained using Axopatch 200B (Axon Instruments, Union City, CA) and a custom data acquisition system written in MATLAB (The MathWorks, Natick, MA) with a sampling rate of either 4 or 10 kHz.

Stimuli. All experiments were conducted in a double-walled sound booth (Industrial Acoustics, Bronx, NY). Free-field stimuli were presented at 97.656 kHz using the TDT System 3 (Tucker-Davis Technologies, Gainesville, FL) connected to an amplifier (STAX SRM-313), which drove a calibrated electrostatic speaker (taken from the left side of a pair of STAX SR-303 headphones) located 8 cm lateral to, and facing, the contralateral (right) ear.

Tone stimuli (100 ms) were presented for 19 neurons (out of 20). Tone protocols consisted of 100-ms long pure-tone pips, 1–48 kHz, 0- to 80-dB sound pressure level (SPL), presented in a fixed pseudorandom order at a rate of 2 tones per second (Hromádka et al. 2008). Natural sound stimuli were presented for 6 neurons (out of 20). The natural sound stimuli were taken from a commercially available audio compact disc, *The Diversity of Animal Sounds* (Cornell Laboratory of Ornithology), originally sampled at 44.1 kHz and resampled at 97.656 kHz for stimulus presentation (Machens et al. 2004). The peak amplitude of each segment was normalized to the ±10-V range of the TDT system, which corresponded to 80-dB SPL.

Analysis of whole cell recordings. Voltage traces were recorded with action potentials superimposed on subthreshold activity. To analyze subthreshold activity, action potentials were removed from raw voltage traces with 4-ms median filter (Jagadeesh et al. 1997). All subthreshold traces shown were median-filtered unless otherwise specified. The resting membrane potential for each trace was defined as the fifth percentile value of the membrane potential across the trace. Nonstationary traces and traces in which the resting membrane potential was above −50 mV were excluded from further analysis.

Recordings analyzed in this manuscript lasted between 2 and 13 min (mean = 7.4 min, median = 7 min, n = 19 neurons), with one additional neuron from which we recorded for ~2 h. Some recordings displayed small and very slow fluctuations in the resting membrane potential. Since we have analyzed 7-s long traces, any small fluctuations in the resting membrane potential on a scale of minutes did not affect the analyses described below. Indeed, the coefficient of variation of the resting membrane potential (for each trace) across all neurons in our sample was 3.95 ± 2.26%, which would correspond to a mean difference of 2.5 mV from trace to trace for a neuron with −60-mV resting potential. One neuron has been used previously as an example in Fig. 2 in DeWeese and Zador (2006).

Kurtosis analysis. For each recorded trace, we computed the kurtosis excess (k) of the membrane voltage distribution (DeWeese and Zador 2006; Olshausen and Field 2004):

$$k = \frac{1}{n}\sum_{i=1}^{n}\frac{(v_i - v_{\text{mean}})^4}{\sigma^4} - 3$$

where n is the number of data points (samples) in a voltage trace, v_i is the membrane potential at data point i, v_{mean} is the mean membrane potential across the trace, and σ is the standard deviation of membrane potential across the trace. For this analysis, we used 7-s long voltage traces (*neurons 2-20*), except for *neuron 1*, for which we recorded data in 4-s long trials.

The kurtosis (we use the term kurtosis instead of kurtosis excess throughout the text) of a normal (Gaussian) distribution is equal to 0. For heavy-tailed distributions, i.e., distributions with tall peaks and long tails, kurtosis is >0.

Note that kurtosis values can be negative. For example, a bimodal distribution consisting of a sum of two Gaussians with means that differ by more than the standard deviation of either Gaussian would result in a negative kurtosis, and in fact we find negative kurtoses for traces from our two PPC neurons that exhibited clear two-state behavior. Kurtosis is negative in this case because the tails fall off faster than a Gaussian with a standard deviation comparable with the separation between the two Gaussian bumps making up the distribution and also because the mean of the distribution falls in the gap between the two Gaussian peaks, so both the tails and the mean are under-represented compared with a single Gaussian fit to the data. Accordingly, we found that negative kurtosis values occurred <5% of the time (31 out of 651 traces) for our auditory-cortex recordings compared with the much higher occurrence of 93% (76 out of 82 traces) for our PPC recordings.

We used kurtosis to measure "sparseness" of subthreshold activity. Occasional deviations from the resting membrane potential (bumps) led to long-tailed distribution of membrane potential values with corresponding kurtosis >0. Note that, because we recorded in awake animals, recordings were more susceptible to pulmonary and cardiac pulsations, recording instabilities, animal movements (e.g., grooming), etc. These events typically lead to a decrease in kurtosis because they smear out the peak of the measured voltage histogram near the resting potential (DeWeese and Zador 2006).

Like kurtosis, skewness (the 3rd standardized moment):

$$s = \frac{1}{n}\sum_{i=1}^{n}\frac{(v_i - v_{\text{mean}})^3}{\sigma^3}$$

could also be used to quantify deviations from Gaussian membrane potential histograms resulting from random walk behavior. We have found, however, that kurtosis distinguishes well between the bimodal histograms characteristic of two-state behavior, even if they are skewed, and the highly kurtotic, unimodal histograms characteristic of traces containing only brief bumps. Moreover, using kurtosis allows

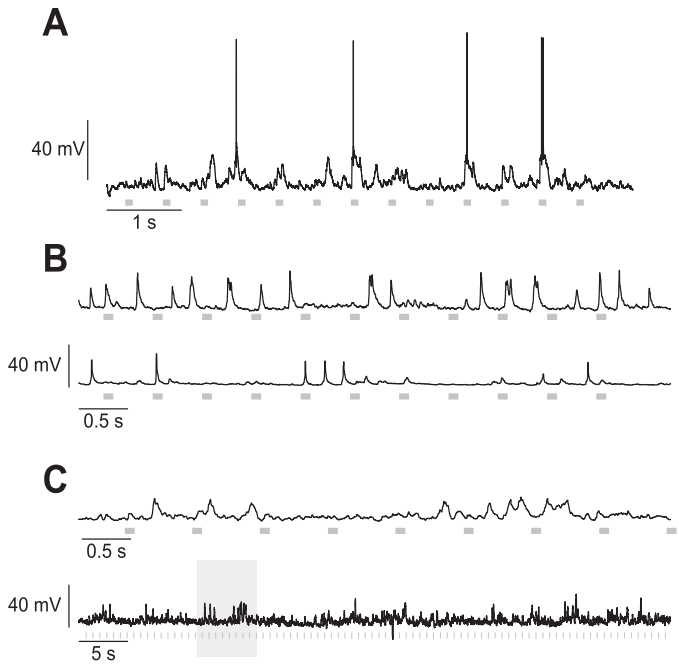

Fig. 1. Subthreshold activity in unanesthetized auditory cortex (ACx) was "bumpy." *A*: example of a voltage trace (7 s) recorded in the ACx of an awake, head-fixed rat. Subthreshold activity consisted of brief excursions of membrane potential, both spontaneous and sound-evoked. *B*: examples of recordings from 2 different neurons demonstrate further that subthreshold dynamics in awake ACx consisted of brief, sporadic fluctuations in membrane potential (bumps). *C*: brief fluctuations were sporadic even on longer time scales. The *top* trace represents a 7-s segment out of a 1-min long trace of subthreshold activity (*bottom*) from a 3rd neuron. The gray rectangle indicates the position of the upper trace. In all panels, small gray bars indicate the positions of the 100-ms tones of different frequencies and intensities.

for a direct comparison of the awake auditory-cortex recordings presented here with our previous analysis of similar recordings from anesthetized animals (DeWeese and Zador 2006).

Dwell-time analysis. Subthreshold membrane potential activity usually appeared as occasional voltage fluctuations above resting membrane potential. We quantified durations of voltage excursions from rest by measuring the amount of time the membrane potential stayed above a given threshold. Excursions separated by gaps <20 ms were merged together as such gaps were considered too brief to separate distinct events. We used absolute thresholds of 10 and 15 mV above resting potential and computed durations of continuous voltage segments above given threshold. For each trace, maximum potential amplitude was defined as the difference between maximum potential and resting membrane potential for the trace. We then also used relative thresholds defined as 20 and 40% of the maximum potential amplitude and computed durations of continuous voltage segments above threshold. The 20% threshold corresponded to 7.33 ± 1.18 mV when expressed in absolute units. Note that such a choice for the threshold is probably quite low (see, for example, Petersen et al. 2003; Stern et al. 1997) and thus may lead to an overestimation of the actual duration of an excursion.

All ranges are given as means $\pm$ standard deviation unless specified otherwise.

RESULTS

To characterize dynamics of membrane potential in the auditory cortex, we used the whole cell patch-clamp technique to record intracellular activity of neurons in the auditory cortex of awake head-fixed rats. Altogether, we recorded from 20 neurons in 13 animals (Sprague-Dawley rats, *postnatal days 24–30*). In addition, as a positive control, we recorded intracellular activity in 2 PPC neurons in the anesthetized preparation.

As in the anesthetized animal, the membrane potential typically remained near the resting level with only occasional large brief excursions [bumps (DeWeese and Zador 2006); Fig. 1]. Classic up states consisting of prolonged depolarizations to a plateau were almost never observed. In what follows, we use the term excursion to include brief and long depolarizations (bumps and up states, respectively), both spontaneous and stimulus-evoked.

We first quantified the statistics of activity by computing the kurtosis (Olshausen and Field 2004; technically, the kurtosis excess; see MATERIALS AND METHODS) of the membrane potential histogram for each recorded trace (Fig. 2). The kurtosis is defined to be 0 for the normal (Gaussian) distribution and is large (>0) for distributions with tall peaks and long tails (Olshausen and Field 2004). Thus if the membrane potential hovers mostly near rest and only occasionally makes large excursions, its histogram will have a tall peak (around rest) and a long tail (corresponding to the excursions), and its kurtosis will be positive.

Individual neurons displayed a wide range of kurtosis values (Fig. 2*A*), from large ones (maximum kurtosis = 2,600 across all traces) corresponding to brief, infrequent bumps (tall histograms with long tails) to small ones (minimum kurtosis = -0.82 across all traces) corresponding to higher activity, which was manifested by a greater number of bumps. *Neuron 9* (Fig. 2*A*) provided the closest example in our data set to a bimodal histogram of membrane potential of the sort associated with canonical up and down states (Anderson et al. 2000; Stern et al. 1997). The dynamics of even this neuron were nonetheless clearly different from the two-state behavior of typical neuron in PPC of an anesthetized rat (Fig. 2*B*) as reflected by its large negative kurtosis (-1.5). We include

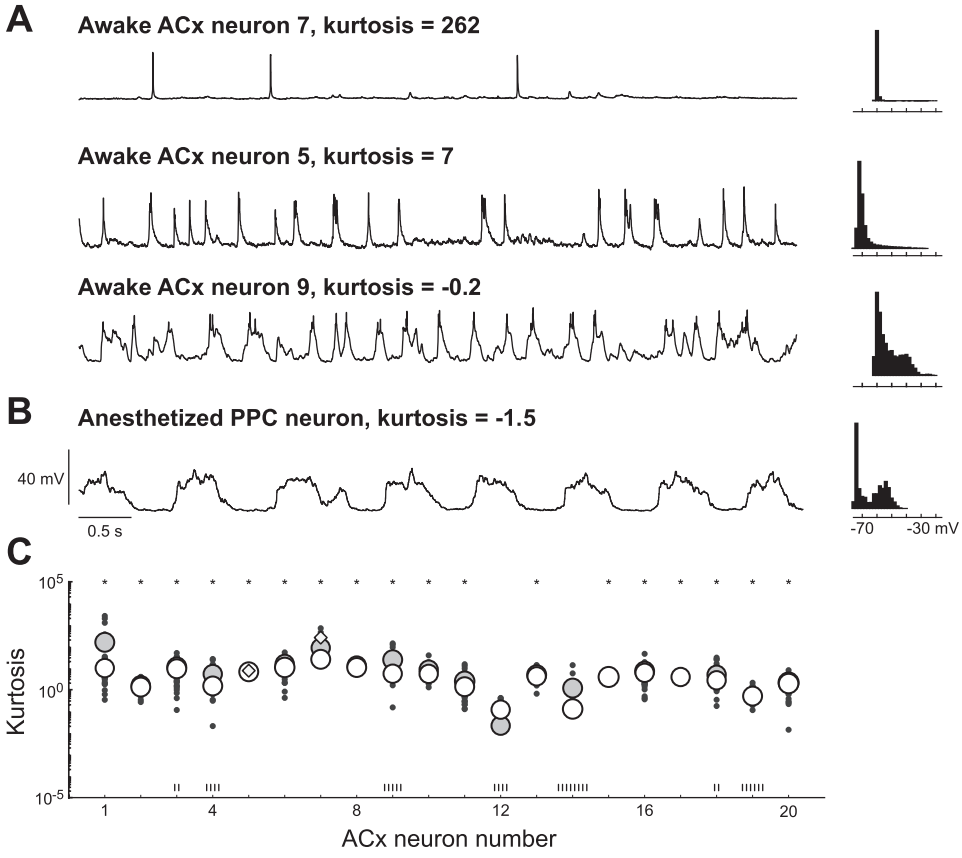

Fig. 2. Kurtoses of recorded traces were usually large and positive, reflecting brief fluctuations of membrane potential. *A*: example traces from 3 different neurons recorded in the unanesthetized ACx exhibited very different kurtoses. Membrane potential distributions for each trace are shown on the *right*. Scale bars are shown in *B*. *B*: traces from a neuron recorded in the posterior parietal cortex (PPC) exhibited 2-state behavior. The membrane potential distribution for this trace is shown on the *right*. *C*: distributions of trace kurtoses (dots), their means (gray), and medians (empty) for 20 neurons. Diamonds correspond to kurtoses of traces from *neurons 5* and *7* in *A*. Note that occasional negative kurtosis values (for example, the trace from *neuron 9* in *A*) are not plotted because of the logarithmic *y*-axis. Number of tick marks at the bottom corresponds to the number of traces with negative kurtosis values for each neuron. Asterisks show neurons with mean kurtoses that were statistically significantly different from 0 (Student's *t*-test, $P < 0.05$).

these example PPC recordings, performed in anesthetized rats, to demonstrate that our electrophysiological technique and kurtosis analysis allow for the detection of two-state behavior when and if it occurs. Overall, kurtoses of subthreshold activity recorded in awake auditory cortex were typically large and positive (Fig. 2*C*; mean = 18, median = 5.6), and negative kurtosis values occurred only 31 times out of 651 traces (5%; vertical tick marks in Fig. 2*C*), indicating that the membrane potential of neurons in awake auditory cortex remained predominantly near rest.

Figure 3 shows the full histograms of membrane potential values for all neurons included in our analysis. Predominantly positive kurtosis values for traces recorded in awake auditory cortex reflected the unimodal nature of membrane voltage distributions with long tails. By contrast, control cells recorded in PPC displayed bimodal distributions of membrane voltage with less prominent tails (resulting mostly in negative kurtosis values), typical for two-state behavior. Although kurtosis values for auditory recordings were typically large, corresponding to bumpy subthreshold dynamics, we have observed lower kurtoses, suggesting occasional wide distributions of membrane potential values for some of the recorded traces (tick marks in Fig. 2*C*) as well as for some neurons when membrane voltage values were pooled (Fig. 3).

Kurtosis, however, is a static measure that cannot distinguish between brief, frequent bumps and long up states. To capture the dynamics of membrane potential, we computed the durations of excursions by assessing the time spent above a given membrane potential threshold (Fig. 4*A*); we used absolute (10 and 15 mV above resting membrane potential) and relative (20 and 40% of maximum potential amplitude) thresholds. This approach is more general than one based either on assuming a bimodal distribution of membrane potentials (Lewis and O'Donnell 2000; Saleem et al. 2010; Stern et al. 1997) or well-isolated bumps (DeWeese and Zador 2006). The lowest relative threshold (20% of maximum amplitude) was always <10 mV and corresponded to 7.33 ± 1.18 mV across all neurons with occasional values as low as 5.24 mV above resting membrane potential. Both 10-mV and 20% thresholds appeared to be lower than thresholds used to compute up-state durations in other in vivo studies (Léger et al. 2005; Stern et al. 1997). Thus the excursion durations computed here are likely to be an overestimate compared with other studies.

The membrane potential spent most of the time near its resting level (i.e., below excursion threshold). Across the population, excursions covered only about 12.5 ± 10% of the recorded traces (10-mV threshold; 21.5 ± 14% for 20% threshold) and were typically brief (Fig. 4), on the order of tens of milliseconds, with few excursions being several hundred milliseconds long. Even for

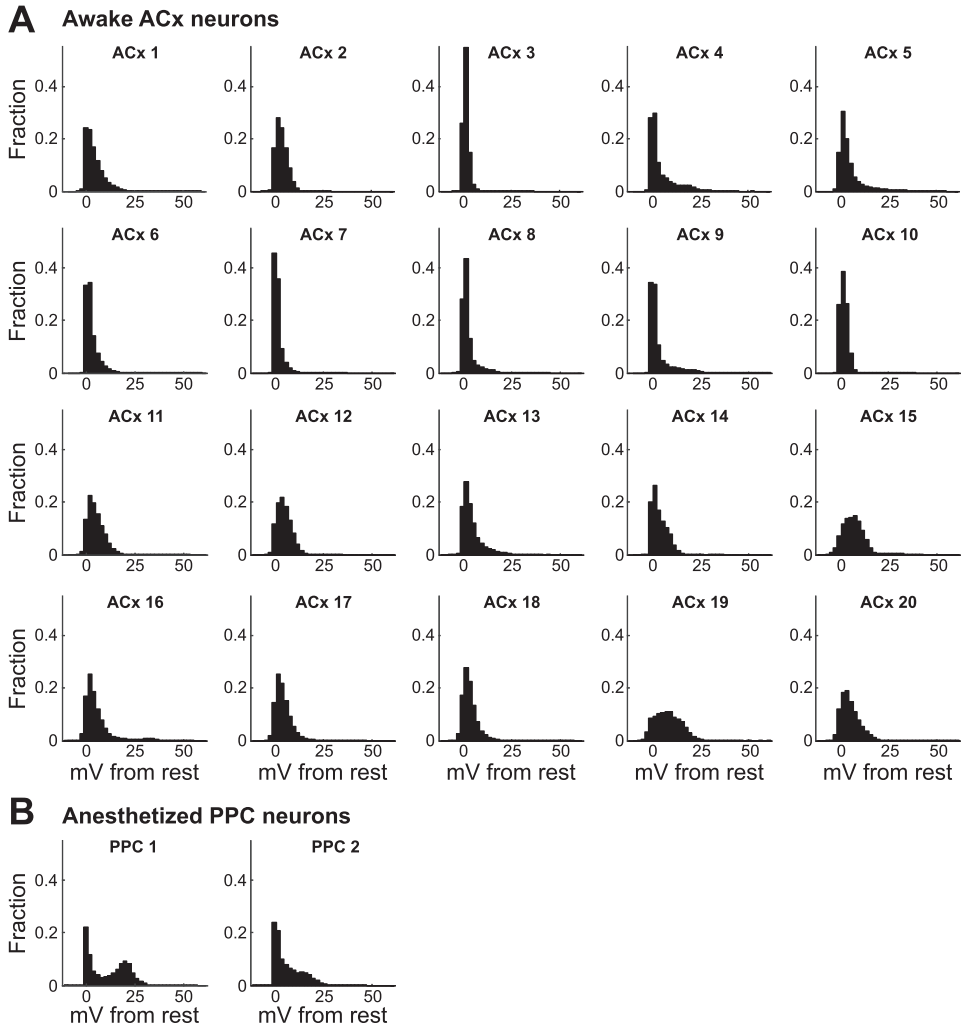

Fig. 3. Membrane voltage histograms of ACx neurons were usually tall with long tails. *A*: plotted are membrane voltage histograms for 20 neurons recorded in the ACx of awake head-fixed rats (ACx 1–20). Membrane voltage histograms for 2 neurons recorded in the PPC of anesthetized rats are plotted in *B* (PPC 1 and PPC 2). Note that whereas neurons recorded in the ACx displayed single-peak histograms, neurons recorded in PPC displayed histograms usually associated with 2-state fluctuations in membrane potential.

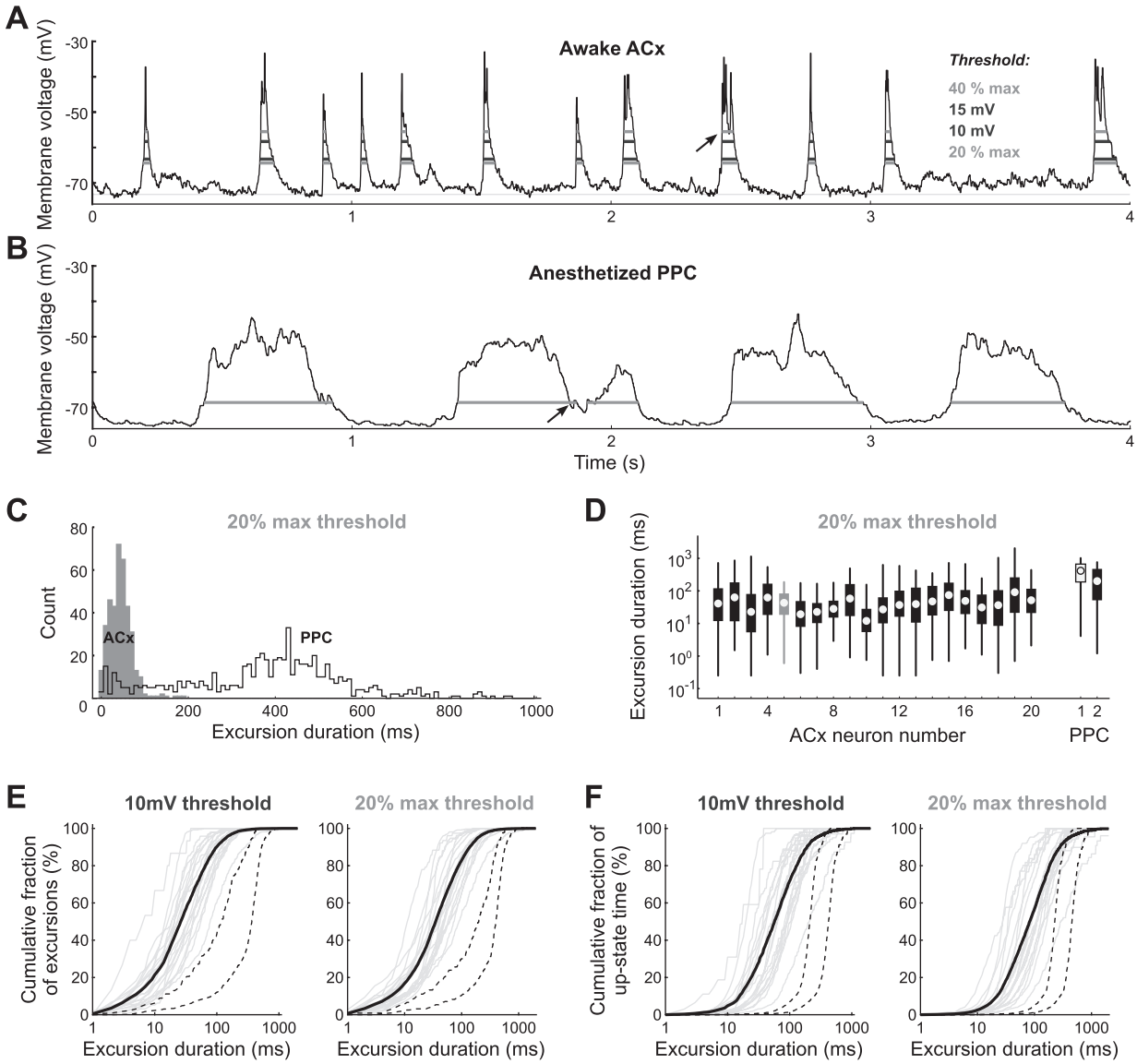

Fig. 4. Membrane potential excursions in awake ACx recordings were brief and rare. *A*: we computed durations of continuous segments (gray horizontal line segments) above a given voltage threshold. Excursions separated by gaps <20 ms were merged (arrow). Thin gray line shows the resting membrane potential. *B*: unambiguous, long up states were evident in this recording from the PPC of an anesthetized rat. Gray horizontal line segments show the 20% maximum (max) threshold for this trace. *C*: histograms of excursion duration for the example ACx neuron shown in *A* and for the example PPC neuron shown in *B*. Excursions for the PPC neuron were up to 1-s long, whereas all excursions for the example ACx neuron were <200 ms (gray). *D*: distributions of excursion durations for 20 ACx neurons and 2 PPC neurons for the lowest threshold (20% max). Circles show median durations for each neuron, boxes extend from 25th to 75th percentile, and whiskers show the total extent of duration values. Gray ACx and empty PPC distributions correspond to distributions of excursion durations for ACx and PPC neurons shown in *A* and *B*, respectively. *E* and *F*: cumulative histograms of excursion duration (*E*) and time spent in up state (*F*) for individual ACx neurons (gray) and population average (thick black line) show that both fraction of excursions >500 ms (*E*) and fraction of time spent in up state (*F*) were very low even for the 2 lowest thresholds. Neurons recorded in PPC are plotted in broken black lines in both panels.

the lowest thresholds, the mean excursion duration across neurons was ~60 ms (60 ± 77 ms, median = 37.5 ms for 20% threshold; 46 ± 56 ms, median = 30 ms for 10-mV threshold). Not surprisingly, excursion durations decreased and fewer excursions were detected for the higher thresholds (29 ± 39 ms, median = 18 ms for 15-mV threshold, and 28 ± 39 ms, median = 18 ms for 40% threshold).

In a few cases, excursions lasted hundreds of milliseconds, up to 1–1.5 s, resembling up states reported in other cortical areas. Such long excursions, however, were very rare with only 0.4% of all excursions >500 ms (48 out of 12,369 excursions, 20% threshold; 0.2%, 15/9,245 for 10-mV threshold; Fig. 4). Individual neurons displayed a range of fractions of short, intermediate bumps and long up states with short bumps (<100 ms) forming >70% of all excursions for most neurons. Furthermore, most time spent away from rest was spent in short bumps; only 0.8% of total recording time was spent in excursions >500 ms (20% threshold; 0.2% for 10-mV threshold). Long excursions (>500 ms) covered, on average, ~3.5% of up-state time (20% threshold; 1.2% for 10-mV threshold) even for the lowest thresholds (Fig. 4) despite being severalfold longer than most of the short excursions.

Altogether, the subthreshold dynamics of traces recorded in awake auditory cortex were consistent with bumpy activity

(Figs. 1 and 2) with few traces displaying behavior consistent with longer up states. Neurons spent most of the time around the resting potential with mostly brief bumps (Fig. 4) and only very rare excursions >500 ms (up states). The majority of excursions were brief even in neurons spending more up-state time in longer excursions, consistent with rapidly changing patterns of membrane potential fluctuations, rather than long up states lasting up to several seconds.

DISCUSSION

We have used whole cell patch-clamp recording in awake head-fixed rats to characterize directly the dynamics of membrane potentials of individual neurons in unanesthetized auditory cortex. Membrane potential dynamics of individual neurons consisted of brief infrequent bumps and only occasionally displayed rapid fluctuations of membrane potential with a few longer up states (excursions >500 ms).

Up and down states were first described in vivo (Cowan and Wilson 1994; Steriade et al. 1993a,b; Wilson and Groves 1981) and subsequently in vitro (Cossart et al. 2003; Sanchez-Vives and McCormick 2000). The bistability of the membrane potential has also been described in vivo in striatum (Kasanetz et al. 2002; Mahon et al. 2003; Stern et al. 1997; Wilson and Kawaguchi 1996) as well as in frontal cortical areas (Léger et al. 2005; Lewis and O'Donnell 2000), somatosensory (Petersen et al. 2003; Sachdev et al. 2004; Steriade et al. 2001; Timofeev et al. 2001), visual (Anderson et al. 2000; Lampl et al. 1999), olfactory (Luo and Katz 2001; Margrie and Schaefer 2003), and other areas (Paré et al. 1998). However, bistability of the membrane potential is not ubiquitous; two states are not always apparent. Brief bumps, such as those described here, have also been described in visual (Anderson et al. 2000; Lampl et al. 1999) and somatosensory (Okun and Lampl 2008; Wilent and Contreras 2005) cortices.

Previous studies have suggested that the presence and characteristics of up and down states depend on the state of vigilance (Mahon et al. 2003). For example, during stimulus-induced cortical desynchronization, a perturbation of the anesthetized animal intended to model a waking state, neurons tend to behave as though in an up state (Kasanetz et al. 2002; Lewis and O'Donnell 2000). Similarly, during the transition from sleeping to waking (Steriade et al. 2001) or from quiet wakefulness to whisking (Crochet and Petersen 2006; Gentet et al. 2010), neurons spent more time in an up state. Here, we found that membrane potential of neurons in the auditory cortex of awake rats remained close to rest in what would elsewhere be characterized as a down state.

Studies of subthreshold activity in auditory cortex of anesthetized animals (DeWeese and Zador 2006; Las et al. 2005; Ojima and Murakami 2002; Tan et al. 2004; Wehr and Zador 2003, 2005; Zhang et al. 2003) and immobilized unanesthetized animals (Ribaupierre et al. 1972; Serkov and Volkov 1984; Volkov and Galaziuk 1985, 1989) are generally consistent with the view that subthreshold activity in the auditory cortex consists mainly of brief and infrequent voltage excursions. However, this conclusion may be somewhat sensitive to the anesthesia used, as membrane dynamics in the urethane-anesthetized auditory cortex displays two-state behavior (Metherate and Ashe 1993), and mean up-state duration is reported to be 200 ms (Saleem et al. 2010).

The dynamics of subthreshold activity in awake (and anesthetized) auditory cortex during both acoustic stimulation and quiet periods can be best described by bumps, i.e., brief, usually infrequent deviations in membrane potential, with only rare excursions >500 ms. We did not observe fast and sustained spiking in most of our neuronal population for the stimuli we presented, leaving open the interesting question of whether strong, sustained responses result from membrane potential dynamics better characterized by many brief bumps in rapid succession or a random walk crossing threshold at many points in time. One neuron in our population, however, displayed brief (mean = 83 ± 76 ms, median = 63 ms; >20% max threshold) excursions underlying periods of brisk firing (mean = 55 ± 69 spikes per second, median = 21 spikes per second) both in response to acoustic stimuli and during periods of silence. These excursions were slightly longer than the bumps we observed in the rest of our auditory-cortex population but still not as long in duration as the up states we observed in our example PPC cells (mean = 334 ± 193 ms, median = 358 ms).

The prevalence of brief bumps in subthreshold activity is consistent with sparse representations (Hromádka et al. 2008) and indicates that single neurons in the auditory cortex receive brief and highly synchronous volleys of activity from their presynaptic partners, unlike neurons in association/visual areas (such as PPC), which seem to receive more persistent synaptic barrages. It is unclear why subthreshold dynamics in auditory cortex would differ from dynamics in other (sensory) cortices, although it is an intriguing possibility that there is an inherent difference between auditory and other sensory areas related to the ability of auditory cortex to exploit fine timing of brief sensory stimuli (Yang et al. 2008).

GRANTS

This work was supported by grants from National Institutes of Health and the Swartz Foundation.

DISCLOSURES

No conflicts of interest, financial or otherwise, are declared by the author(s).

AUTHOR CONTRIBUTIONS

T.H., A.M.Z., and M.R.D. conception and design of research; T.H. and M.R.D. performed experiments; T.H. analyzed data; T.H., A.M.Z., and M.R.D. interpreted results of experiments; T.H. prepared figures; T.H. drafted manuscript; T.H., A.M.Z., and M.R.D. edited and revised manuscript; T.H., A.M.Z., and M.R.D. approved final version of manuscript.

REFERENCES

Anderson J, Lampl I, Reichova I, Carandini M, Ferster D. Stimulus dependence of two-state fluctuations of membrane potential in cat visual cortex. *Nat Neurosci* 3: 617–621, 2000.

Bruno RM, Sakmann B. Cortex is driven by weak but synchronously active thalamocortical synapses. *Science* 312: 1622–1627, 2006.

Carandini M, Ferster D. A tonic hyperpolarization underlying contrast adaptation in cat visual cortex. *Science* 276: 949–952, 1997.

Cossart R, Aronov D, Yuste R. Attractor dynamics of network up states in the neocortex. *Nature* 423: 283–288, 2003.

Cowan RL, Wilson CJ. Spontaneous firing patterns and axonal projections of single corticostriatal neurons in the rat medial agranular cortex. *J Neurophysiol* 71: 17–32, 1994.

Crochet S, Petersen CC. Correlating whisker behavior with membrane potential in barrel cortex of awake mice. *Nat Neurosci* 9: 608–610, 2006.

DeWeese MR, Wehr M, Zador AM. Binary spiking in auditory cortex. *J Neurosci* 23: 7940–7949, 2003.

DeWeese MR, Zador AM. Non-Gaussian membrane potential dynamics imply sparse, synchronous activity in auditory cortex. *J Neurosci* 26: 12206–12218, 2006.

Doron N, Ledoux J, Semple M. Redefining the tonotopic core of rat auditory cortex: physiological evidence for a posterior field. *J Comp Neurol* 453: 345–360, 2002.

Gentet LJ, Avermann M, Matyas F, Staiger JF, Petersen CC. Membrane potential dynamics of GABAergic neurons in the barrel cortex of behaving mice. *Neuron* 65: 422–435, 2010.

Haslinger R, Ulbert I, Moore CI, Brown EN, Devor A. Analysis of LFP phase predicts sensory response of barrel cortex. *J Neurophysiol* 96: 1658–1663, 2006.

Hromádka T, Deweese MR, Zador AM. Sparse representation of sounds in the unanesthetized auditory cortex. *PLoS Biol* 6: e16, 2008.

Jagadeesh B, Wheat HS, Kontsevich LL, Tyler CW, Ferster D. Direction selectivity of synaptic potentials in simple cells of the cat visual cortex. *J Neurophysiol* 78: 2772–2789, 1997.

Kasanetz F, Riquelme LA, Murer MG. Disruption of the two-state membrane potential of striatal neurones during cortical desynchronisation in anaesthetised rats. *J Physiol* 543: 577–589, 2002.

Lampl I, Reichova I, Ferster D. Synchronous membrane potential fluctuations in neurons of the cat visual cortex. *Neuron* 22: 361–374, 1999.

Las L, Stern EA, Nelken I. Representation of tone in fluctuating maskers in the ascending auditory system. *J Neurosci* 25: 1503–1513, 2005.

Léger J, Stern EA, Aertsen A, Heck D. Synaptic integration in rat frontal cortex shaped by network activity. *J Neurophysiol* 93: 281–293, 2005.

Lewis BL, O'Donnell P. Ventral tegmental area afferents to the prefrontal cortex maintain membrane potential 'up' states in pyramidal neurons via D(1) dopamine receptors. *Cereb Cortex* 10: 1168–1175, 2000.

Luczak A, Bartho P, Marguet SL, Buzsaki G, Harris KD. Sequential structure of neocortical spontaneous activity in vivo. *Proc Natl Acad Sci USA* 104: 347–352, 2007.

Luo M, Katz LC. Response correlation maps of neurons in the mammalian olfactory bulb. *Neuron* 32: 1165–1179, 2001.

Machens CK, Wehr MS, Zador AM. Linearity of cortical receptive fields measured with natural sounds. *J Neurosci* 24: 1089–1100, 2004.

Mahon S, Deniau J, Charpier S. Various synaptic activities and firing patterns in cortico-striatal and striatal neurons in vivo. *J Physiol (Paris)* 97: 557–566, 2003.

Margrie TW, Schaefer AT. Theta oscillation coupled spike latencies yield computational vigour in a mammalian sensory system. *J Physiol* 546: 363–374, 2003.

McCormick DA, Shu Y, Hasenstaub A, Sanchez-Vives M, Badoual M, Bal T. Persistent cortical activity: mechanisms of generation and effects on neuronal excitability. *Cereb Cortex* 13: 1219–1231, 2003.

Metherate R, Ashe JH. Ionic flux contributions to neocortical slow waves and nucleus basalis-mediated activation: whole-cell recordings in vivo. *J Neurosci* 13: 5312–5323, 1993.

Nakamura K. Auditory spatial discriminatory and mnemonic neurons in rat posterior parietal cortex. *J Neurophysiol* 82: 2503–2517, 1999.

Ojima H, Murakami K. Intracellular characterization of suppressive responses in supragranular pyramidal neurons of cat primary auditory cortex in vivo. *Cereb Cortex* 12: 1079–1091, 2002.

Okun M, Lampl I. Instantaneous correlation of excitation and inhibition during ongoing and sensory-evoked activities. *Nat Neurosci* 11: 535–537, 2008.

Okun M, Naim A, Lampl I. The subthreshold relation between cortical local field potential and neuronal firing unveiled by intracellular recordings in awake rats. *J Neurosci* 30: 4440–4448, 2010.

Olshausen BA, Field DJ. Sparse coding of sensory inputs. *Curr Opin Neurobiol* 14: 481–487, 2004.

Paré D, Shink E, Gaudreau H, Destexhe A, Lang EJ. Impact of spontaneous synaptic activity on the resting properties of cat neocortical pyramidal neurons in vivo. *J Neurophysiol* 79: 1450–1460, 1998.

Petersen CC, Hahn TT, Mehta M, Grinvald A, Sakmann B. Interaction of sensory responses with spontaneous depolarization in layer 2/3 barrel cortex. *Proc Natl Acad Sci USA* 100: 13638–13643, 2003.

Ribaupierre FD, Goldstein MH, Yeni-Komshian G. Intracellular study of the cat's primary auditory cortex. *Brain Res* 48: 185–204, 1972.

Sachdev RN, Ebner FF, Wilson CJ. Effect of subthreshold up and down states on the whisker-evoked response in somatosensory cortex. *J Neurophysiol* 92: 3511–3521, 2004.

Saleem AB, Chadderton P, Apergis-Schoute J, Harris KD, Schultz SR. Methods for predicting cortical up and down states from the phase of deep layer local field potentials. *J Comput Neurosci* 29: 49–62, 2010.

Sanchez-Vives MV, McCormick DA. Cellular and network mechanisms of rhythmic recurrent activity in neocortex. *Nat Neurosci* 3: 1027–1034, 2000.

Serkov F, Volkov I. Intracellular reactions of neurons of the primary auditory area of the cerebral cortex in the cat to tones of different frequency and electric stimulation of nerve fibers of the spiral ganglion. *Neirofiziologiia* 16: 123–131, 1984.

Steriade M, Nuñez A, Amzica F. A novel slow (<1 Hz) oscillation of neocortical neurons in vivo: depolarizing and hyperpolarizing components. *J Neurosci* 13: 3252–3265, 1993a.

Steriade M, Nuñez A, Amzica F. Intracellular analysis of relations between the slow (<1 Hz) neocortical oscillation and other sleep rhythms of the electroencephalogram. *J Neurosci* 13: 3266–3283, 1993b.

Steriade M, Timofeev I, Grenier F. Natural waking and sleep states: a view from inside neocortical neurons. *J Neurophysiol* 85: 1969–1985, 2001.

Stern EA, Kincaid AE, Wilson CJ. Spontaneous subthreshold membrane potential fluctuations and action potential variability of rat corticostriatal and striatal neurons in vivo. *J Neurophysiol* 77: 1697–1715, 1997.

Tan AY, Zhang LI, Merzenich MM, Schreiner CE. Tone-evoked excitatory and inhibitory synaptic conductances of primary auditory cortex neurons. *J Neurophysiol* 92: 630–643, 2004.

Timofeev I, Grenier F, Steriade M. Disfacilitation and active inhibition in the neocortex during the natural sleep-wake cycle: an intracellular study. *Proc Natl Acad Sci USA* 98: 1924–1929, 2001.

Volkov I, Galaziuk A. Reactions of neurons of the auditory cortex of unanesthetized cats to tones of a characteristic frequency. *Neirofiziologiia* 17: 500–508, 1985.

Volkov I, Galaziuk A. Reactions of tonic-type neurons in the cat auditory cortex to tones of various frequency and intensity. *Neirofiziologiia* 21: 498–506, 1989.

Wang XJ. Synaptic reverberation underlying mnemonic persistent activity. *Trends Neurosci* 24: 455–463, 2001.

Wehr M, Zador AM. Balanced inhibition underlies tuning and sharpens spike timing in auditory cortex. *Nature* 426: 442–446, 2003.

Wehr M, Zador AM. Synaptic mechanisms of forward suppression in rat auditory cortex. *Neuron* 47: 437–445, 2005.

Wilent WB, Contreras D. Dynamics of excitation and inhibition underlying stimulus selectivity in rat somatosensory cortex. *Nat Neurosci* 8: 1364–1370, 2005.

Wilson CJ, Groves PM. Spontaneous firing patterns of identified spiny neurons in the rat neostriatum. *Brain Res* 220: 67–80, 1981.

Wilson CJ, Kawaguchi Y. The origins of two-state spontaneous membrane potential fluctuations of neostriatal spiny neurons. *J Neurosci* 16: 2397–2410, 1996.

Yang Y, DeWeese MR, Otazu GH, Zador AM. Millisecond-scale differences in neural activity in auditory cortex can drive decisions. *Nat Neurosci* 11: 1262–1263, 2008.

Zhang LI, Tan AY, Schreiner CE, Merzenich MM. Topography and synaptic shaping of direction selectivity in primary auditory cortex. *Nature* 424: 201–205, 2003.